Preprints (www.preprints.org) | NOT PEER-REVIEWED | Posted: 31 January 2023 doi:10.20944/preprints202301.0581.v1

Disclaimer/Publisher's Note: The statements, opinions, and data contained in all publications are solely those of the individual author(s) and contributor(s) and not of MDPI and/or the editor(s). MDPI and/or the editor(s) disclaim responsibility for any injury to people or property resulting from any ideas, methods, instructions, or products referred to in the content.

Article

Development of a Novel Anti-CD44 Variant 5 Monoclonal Antibody C44Mab-3 for Multiple Applications against Pancreatic Carcinomas

Yuma Kudo [1], Hiroyuki Suzuki [1,2]*, Tomohiro Tanaka [1,2], Mika K. Kaneko [1,2] and Yukinari Kato [1,2]*

[1] Department of Molecular Pharmacology, Tohoku University Graduate School of Medicine, 2-1 Seiryo-machi, Aoba-ku, Sendai 980-8575, Miyagi, Japan; kudo.yuma.p4@dc.tohoku.ac.jp (Y.Kudo); tomohiro.tanaka.b5@tohoku.ac.jp (T.T.)

[2] Department of Antibody Drug Development, Tohoku University Graduate School of Medicine, 2-1 Seiryo-machi, Aoba-ku, Sendai 980-8575, Miyagi, Japan; k.mika@med.tohoku.ac.jp (M.K.K.)

* Correspondence: hiroyuki.suzuki.b4@tohoku.ac.jp (H. S.); yukinari.kato.e6@tohoku.ac.jp (Y.Kato); Tel.: +81-29-853-3944 (H.S., Y.Kato)

Abstract: Pancreatic cancer exhibits a poor prognosis due to the lack of early diagnostic biomarkers and the resistance to conventional chemotherapy. CD44 has been known as a cancer stem cell marker, and plays tumor promotion and drug resistance in various cancers. Especially, the splicing variants are overexpressed in many carcinomas, and play essential roles in the cancer stemness, invasiveness or metastasis, and resistance to treatments. Therefore, the understanding of each CD44 variant (CD44v) function and distribution in carcinomas is essential for the establishment of CD44-targeting tumor therapy. In this study, we immunized mice with CD44v3–10-overexpressed Chinese hamster ovary-K1 (CHO) cells, and established various anti-CD44 monoclonal antibodies (mAbs). One of the established clones (C44Mab-3; IgG_1, kappa) recognized peptides of the variant 5-encoded region, indicating that C44Mab-3 is a specific mAb for CD44v5. Moreover, C44Mab-3 reacted with CHO/CD44v3–10 cells or pancreatic cancer cell lines (PK-1 and PK-8) by flow cytometry. The apparent K_D of C44Mab-3 for CHO/CD44v3–10 and PK-1 was 7.1×10^{-10} M and 1.9×10^{-9} M, respectively. C44Mab-3 could detect the exogenous CD44v3–10 and endogenous CD44v5 in western blotting, and stained the formalin-fixed paraffin-embedded pancreatic cancer cells, but not normal pancreatic epithelial cells in immunohistochemistry. These results indicate that C44Mab-3 is useful for detecting CD44v5 in various applications, and expected for the application of pancreatic cancer diagnosis and therapy.

Keywords: CD44; CD44 variant 5; monoclonal antibody; flow cytometry; immunohistochemistry

1. Introduction

Pancreatic cancer has become the third leading cause of death in men and women combined in United States, 2022 [1]. The development of pancreatic cancer has been explained by four common oncogenic events, including *KRAS, CDKN2A, SMAD4,* and *TP53* [2,3]. However, pancreatic cancer shows the heterogeneity in drug response and clinical outcomes [4]. Therefore, the detailed understanding of pancreatic cancers has been required to improve patient selection for current therapies, and to develop novel therapeutic strategies. An integrated genomic analysis of pancreatic ductal adenocarcinomas (PDAC) was performed and defined four subtypes, including squamous, pancreatic progenitor, immunogenic, and aberrantly differentiated endocrine exocrine (ADEX), which correspond to the histopathological characteristics [5]. Additionally, various marker proteins have been investigated for early diagnostic and drug responses of pancreatic cancers [6,7]. Studies have suggested that CD44 plays important roles in malignant progression of tumors through its cancer stemness and metastasis-promoting properties [8].

© 2023 by the author(s). Distributed under a Creative Commons CC BY license.

Preprints (www.preprints.org) | NOT PEER-REVIEWED | Posted: 31 January 2023 doi:10.20944/preprints202301.0581.v1

CD44 is a type I transmembrane glycoprotein, and is expressed as a wide variety of isoforms in various type of cells. [9]. The variety of isoforms is produced by the alternative splicing of CD44 mRNA. The CD44 standard isoform (CD44s) is the smallest isoform of CD44 (85–95 kDa), which presents on the membrane of most vertebrate cells. CD44s mRNA is assembled by the first five and the last five constant region exons [10]. The CD44 variant isoforms (CD44v) are produced by the alternative splicing of middle variant exons (v1–v10) and the standard exons of CD44s [11]. Both CD44s and CD44v (pan-CD44) are known as hyaluronic acid (HA) receptor, which mediates cellular homing, migration, adhesion, and proliferation [12,13].

CD44v isoforms were overexpressed in carcinomas and induced metastatic properties [14,15]. A growing body of evidence suggests that CD44v plays critical roles in the promotion of tumor invasion, metastasis, cancer-initiating properties [16], and resistance to chemo- and radiotherapy [17,18]. Reports indicated the important functions of each variant exon-encoded region. The v3-encoded region acts as a co-receptor of receptor tyrosine kinases [19]. Since the v3-encoded region possesses heparan sulfate moieties, it can recruit to fibroblast growth factors (FGFs) and heparin-binding epidermal growth factor-like growth factor (HB-EGF). Furthermore, the v6-encoded region forms ternary complex with HGF and its receptor c-MET, which is essential for the activation [20]. Additionally, the oxidative stress resistance is mediated by the v8–10-encoded region through binding with a cystine–glutamate transporter (xCT) subunit [21]. Therefore, establishment and characterization of mAbs, which recognize each CD44v, are thought to be essential for understanding each variant function and development of CD44-targeting tumor diagnosis and therapy. However, the function and distribution of the variant 5-encoded region in tumors have not been fully understood.

Our group established the novel anti-pan-CD44 mAbs, C$_{44}$Mab-5 (IgG$_1$, kappa) [22] and C$_{44}$Mab-46 (IgG$_1$, kappa) [23] using the Cell-Based Immunization and Screening (CBIS) method and immunization of CD44v3–10 ectodomain, respectively. Both C$_{44}$Mab-5 and C$_{44}$Mab-46 have epitopes within the standard exons (1 to 5)-encoding sequences [24-26]. Furthermore, we showed that both C$_{44}$Mab-5 and C$_{44}$Mab-46 are applicable to flow cytometry and immunohistochemistry in oral [22] and esophageal squamous cell carcinomas (SCC) [23]. We have also investigated the antitumor effects of core-fucose deficient C$_{44}$Mab-5 in mouse xenograft models of oral SCC [27]. Here, we developed a novel anti-CD44v5 mAb, C$_{44}$Mab-3 (IgG$_1$, kappa) by CBIS method, and assessed its applications, including flow cytometry, western blotting, and immunohistochemical analyses.

2. Materials and Methods

2.1. Cell lines

CHO-K1 and mouse multiple myeloma P3X63Ag8U.1 (P3U1) cell lines were obtained from the American Type Culture Collection (ATCC, Manassas, VA, USA). Human pancreas cancer cell lines, PK-1 and PK-8 were obtained from the Cell Resource Center for Biomedical Research Institute of Development, Aging and Cancer at Tohoku University. These cells were cultured in Roswell Park Memorial Institute (RPMI)-1640 medium (Nacalai Tesque, Inc., Kyoto, Japan), supplemented with 100 U/mL penicillin, 100 μg/mL streptomycin, 0.25 μg/mL amphotericin B (Nacalai Tesque, Inc.), and 10% heat-inactivated fetal bovine serum (FBS; Thermo Fisher Scientific, Inc., Waltham, MA, USA). All the cells were grown in a humidified incubator at 37°C with 5% CO_2.

2.2. Plasmid construction and establishment of stable transfectants

CD44v3–10 open reading frame was obtained from the RIKEN BRC through the National Bio-Resource Project of the MEXT, Japan. CD44s cDNA was amplified using HotStar HiFidelity Polymerase Kit (Qiagen Inc., Hilden, Germany) using LN229 (a glioblastoma cell line) cDNA as a template. CD44v3–10 and CD44 cDNAs were cloned into pCAG-Ble-ssPA16 vector with signal sequence and N-terminal PA16 tag of 16 amino acids (GLEGGVAMPGAEDDVV) [22,28-31], which is detected by NZ-1, which was originally

Preprints (www.preprints.org) | NOT PEER-REVIEWED | Posted: 31 January 2023 doi:10.20944/preprints202301.0581.v1

developed against human podoplanin [32-47]. The pCAG-Ble/PA16-CD44s and pCAG-Ble/PA16-CD44v3–10 vectors were transfected into CHO-K1 cells using a Neon transfection system (Thermo Fisher Scientific, Inc.), which offers an innovative electroporation method that utilizes a proprietary biologically compatible pipette tip chamber to generate a more uniform electric field for a significant increase in transfection efficiency and cell viability. By limiting dilution method, CHO/CD44s and CHO/CD44v3–10 clones were finally established.

2.3. Hybridomas

The female BALB/c mice were purchased from CLEA Japan (Tokyo, Japan). Animals were housed under specific pathogen-free conditions. All animal experiments were also conducted according to relevant guidelines and regulations to minimize animal suffering and distress in the laboratory. The Animal Care and Use Committee of Tohoku University (Permit number: 2019NiA-001) approved animal experiments. The mice were monitored daily for health during the full four-week duration of the experiment. A reduction of more than 25% of the total body weight was defined as a humane endpoint. During sacrifice, the mice were euthanized through cervical dislocation, after which death was verified through respiratory and cardiac arrest. BALB/c mice were intraperitoneally immunized with CHO/CD44v3–10 (1×10^8 cells) and Imject Alum (Thermo Fisher Scientific Inc.) as an adjuvant, which stimulates a nonspecific immune response for mixed antigens using this formulation of aluminum hydroxide and magnesium hydroxide. After the three additional immunizations per week, a booster injection was performed two days before harvesting the spleen cells of immunized mice. The hybridomas were established by the fusion of splenocytes and P3U1 cells using polyethylene glycol 1500 (PEG1500; Roche Diagnostics, Indianapolis, IN, USA). RPMI-1640 supplemented with hypoxanthine, aminopterin, and thymidine (HAT; Thermo Fisher Scientific Inc.) was used for the selection of hybridomas. The supernatants, which are positive for CHO/CD44v3–10 cells and negative for CHO-K1 cells, were selected by the flow cytometry-based high throughput screening using SA3800 Cell Analyzers (Sony Corp. Tokyo, Japan).

2.4. Enzyme-linked immunosorbent assay (ELISA)

Fifty-eight synthesized peptides, which cover the CD44v3–10 extracellular domain [24], were synthesized by Sigma-Aldrich Corp. (St. Louis, MO, USA) The peptides (1 μg/mL) were immobilized on Nunc Maxisorp 96-well immunoplates (Thermo Fisher Scientific Inc) for 30 min at 37°C. After washing with phosphate-buffered saline (PBS) containing 0.05% (*v*/*v*) Tween 20 (PBST; Nacalai Tesque, Inc.) using Microplate Washer, HydroSpeed (Tecan, Zürich, Switzerland), wells were blocked with 1% (*w*/*v*) bovine serum albumin (BSA)-containing PBST for 30 min at 37°C. C_{44}Mab-3 (10 μg/mL) were added to each well, and then incubated with anti-mouse immunoglobulins conjugated to peroxidase (1:2000 diluted; Agilent Technologies Inc., Santa Clara, CA, USA). Enzymatic reactions were performed using 1-Step Ultra TMB (Thermo Fisher Scientific Inc.). The optical density (655 nm) was mesured using an iMark microplate reader (Bio-Rad Laboratories, Inc., Berkeley, CA, USA).

2.5. Flow cytometry

CHO-K1, CHO/CD44v3–10, PK-1, and PK-8 were harvested using 0.25% trypsin and 1 mM ethylenediamine tetraacetic acid (EDTA; Nacalai Tesque, Inc.). The cells were treated with C_{44}Mab-3, C_{44}Mab-46, or blocking buffer (control) (0.1% bovine serum albumin [BSA; Nacalai Tesque, Inc.] in PBS) for 30 min at 4°C. Then, the cells were treated with Alexa Fluor 488-conjugated anti-mouse IgG (1:2000; Cell Signaling Technology, Inc.) for 30 min at 4°C. Fluorescence data were collected using the SA3800 Cell Analyzer and analyzed using SA3800 software ver. 2.05 (Sony Corporation).

Preprints (www.preprints.org) | NOT PEER-REVIEWED | Posted: 31 January 2023 doi:10.20944/preprints202301.0581.v1

2.6. Determination of dissociation constant (K_D) via flow cytometry

Serially diluted C44Mab-3 was treated with CHO/CD44v3–10 and PK-1 cells. The cells were further incubated with Alexa Fluor 488-conjugated anti-mouse IgG (1:200). Fluorescence data were collected using BD FACSLyric and analyzed using BD FACSuite software version 1.3 (BD Biosciences). The dissociation constant (K_D) was determined by GraphPad Prism 8 (the fitting binding isotherms to built-in one-site binding models; GraphPad Software, Inc., La Jolla, CA, USA).

2.7. Western blot analysis

The total cell lysates (10 μg of protein) were subjected to electrophoresis on polyacrylamide gels (5%–20% gel, FUJIFILM Wako Pure Chemical Corporation, Osaka, Japan). The separated proteins were transferred onto polyvinylidene difluoride (PVDF) membranes (Merck KGaA, Darmstadt, Germany). The blocking was performed using 4% skim milk (Nacalai Tesque, Inc.) in PBS with 0.05% Tween 20. The membranes were incubated with 10 μg/mL of C44Mab-3, 10 μg/mL of C44Mab-46, 0.5 μg/mL of NZ-1, or 1 μg/mL of an anti-β-actin mAb (clone AC-15; Sigma-Aldrich Corp.), and then incubated with peroxidase-conjugated anti-mouse immunoglobulins (diluted 1:1000; Agilent Technologies, Inc.) for C44Mab-3, C44Mab-46, and anti-β-actin. The anti-rat immunoglobulins (diluted 1:1000; Agilent Technologies, Inc.) conjugated with peroxidase was used for NZ-1. The chemiluminescence signals were obtained with ImmunoStar LD (FUJIFILM Wako Pure Chemical Corporation), and detected using a Sayaca-Imager (DRC Co. Ltd., Tokyo, Japan).

2.8. Immunohistochemical analysis

One formalin-fixed paraffin-embedded (FFPE) oral SCC tissue was obtained from Tokyo Medical and Dental University [48]. FFPE sections of pancreatic carcinoma tissue arrays (Catalog number: PA241c and PA484) were purchased from US Biomax Inc. (Rockville, MD, USA). Pancreas adenocarcinoma tissue microarray with adjacent normal pancreas tissue (PA241c) contains 6 cases of pancreas adenocarcinoma with matched adjacent normal pancreas tissue, quadruple cores per case. Pancreas adenocarcinoma tissue microarray (PA484) contains 18 cases of pancreas adenocarcinoma, 1 each of pancreas islet cell tumor, mucinous adenocarcinoma and undifferentiated carcinoma, plus 3 normal pancreas tissue, duplicate cores per case. One oral SCC tissue was autoclaved in citrate buffer (pH 6.0; Nichirei biosciences, Inc., Tokyo, Japan), and pancreatic carcinoma tissue arrays were autoclaved in EnVision FLEX Target Retrieval Solution High pH (Agilent Technologies, Inc.) for 20 min. After blocking with SuperBlock T20 (Thermo Fisher Scientific, Inc.), the sections were incubated with C44Mab-3 (1 μg/mL) and C44Mab-46 (1 μg/mL) for 1 h at room temperature and then treated with the EnVision+ Kit for mouse (Agilent Technologies Inc.) for 30 min. The color was developed using 3,3′-diaminobenzidine tetrahydrochloride (DAB; Agilent Technologies Inc.). Hematoxylin (FUJIFILM Wako Pure Chemical Corporation) was used for the counterstaining. Leica DMD108 (Leica Microsystems GmbH, Wetzlar, Germany) was used to examine the sections and obtain images.

3. Results

3.1. Development of an anti-CD44v5 mAb, C44Mab-3

In the CBIS method, we used a stable transfectant (CHO/CD44v3–10 cells) as an immunogen (Figure. 1). Mice were immunized with CHO/CD44v3–10 cells, and hybridomas were seeded into 96-well plates. The supernatants, which are positive for CHO/CD44v3–10 cells and negative for CHO-K1 cells, were selected using the flow cytometry-based high throughput screening. By limiting dilution, anti-CD44 mAb-producing clones were finally established. Among them, C44Mab-3 (IgG_1, kappa) was shown to recognize both CD44p311–330 (AYEGNWNPEAHPPLIHHEHH) and CD44p321–340 peptides (HPPLIHHEHHEEEETPHSTS), which are corresponding to variant 5-encoded sequence (supplementary Table S1).

Preprints (www.preprints.org) | NOT PEER-REVIEWED | Posted: 31 January 2023 doi:10.20944/preprints202301.0581.v1

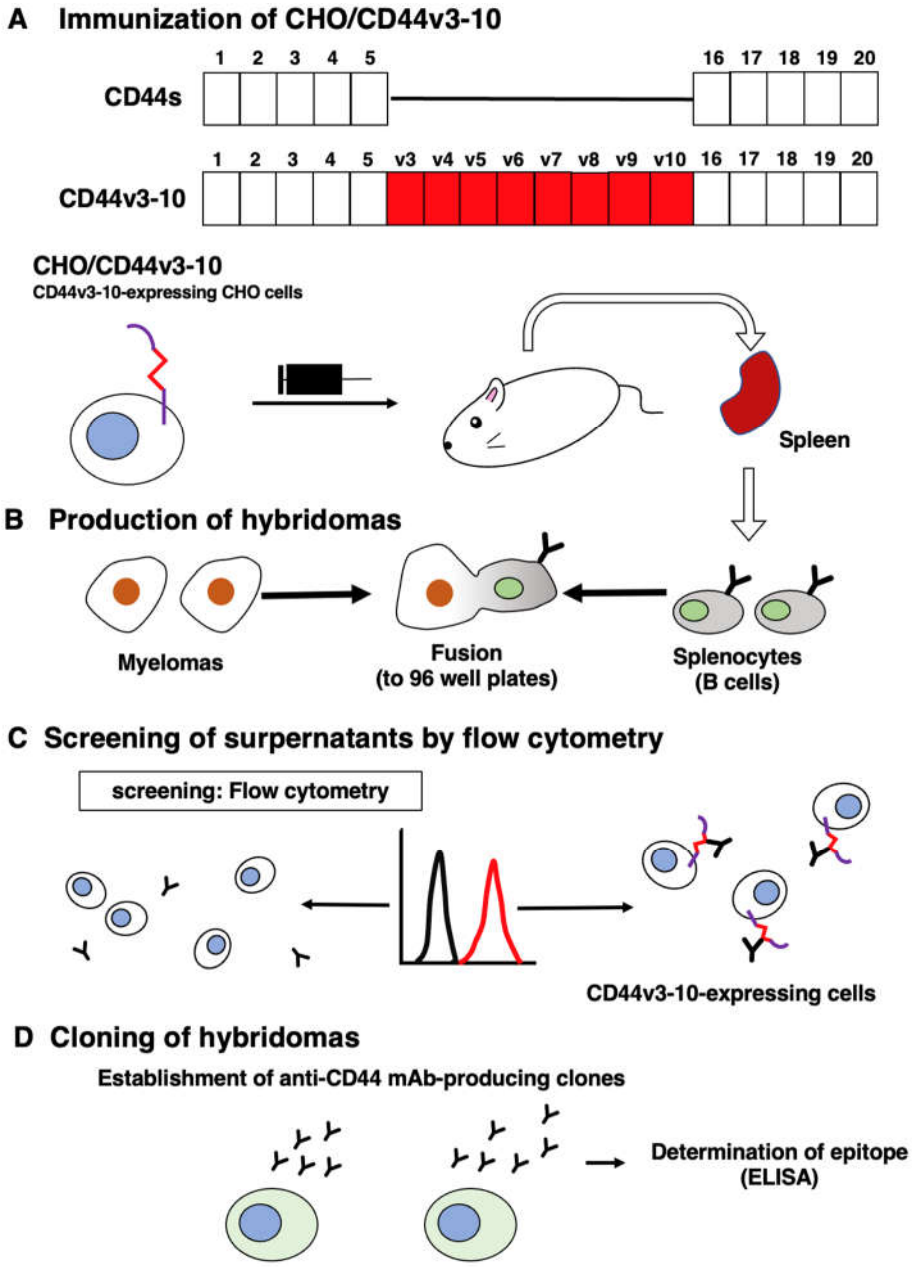

Figure 1. A schematic illustration of ant-human CD44 mAbs production. **(A)** CHO/CD44v3–10 cells were intraperitoneally injected into BALB/c mice. **(B)** Hybridomas were produced by fusion of the splenocytes and P3U1 cells **(C)** The screening was performed by flow cytometry using parental CHO-K1 and CHO/CD44v3–10 cells. **(D)** After cloning and additional screening, a clone C$_{44}$Mab-3 (IgG$_1$, kappa) was established. Furthermore, the binding epitopes were determined by enzyme-linked immunosorbent assay (ELISA) using peptides, which cover the extracellular domain of CD44v3–10.

3.2. Flow Cytometry using C$_{44}$Mab-3 to CD44-Expressing Cells

We next investigated the reactivity of C$_{44}$Mab-3 against CHO/CD44v3–10, CHO/CD44s, and CHO-K1 cells by flow cytometry. C$_{44}$Mab-3 recognized CHO/CD44v3–10 cells in a dose-dependent manner (Figure 2A), but neither CHO/CD44s (Figure 2B) nor CHO-K1 (Figure 2C) cells. The CHO/CD44s cells were recognized by an anti-pan-CD44 mAb C$_{44}$Mab-46 [23] (Supplemental Figure S1). Furthermore, C$_{44}$Mab-3 also recognized pancreatic cancer cell lines, such as PK-1 (Figure 2D) and PK-8 (Figure 2E) in a dose-dependent manner.

Preprints (www.preprints.org) | NOT PEER-REVIEWED | Posted: 31 January 2023 doi:10.20944/preprints202301.0581.v1

We next determined the apparent binding affinity of C44Mab-3 with CHO/CD44v3–10 and PK-1 using flow cytometry. The K_D of CHO/CD44v3–10 and PK-1 was 7.1×10^{-10} M and 1.9×10^{-9} M, respectively, indicating that C44Mab-3 possesses high affinity for CD44v3–10-expressing cells (Figure 3).

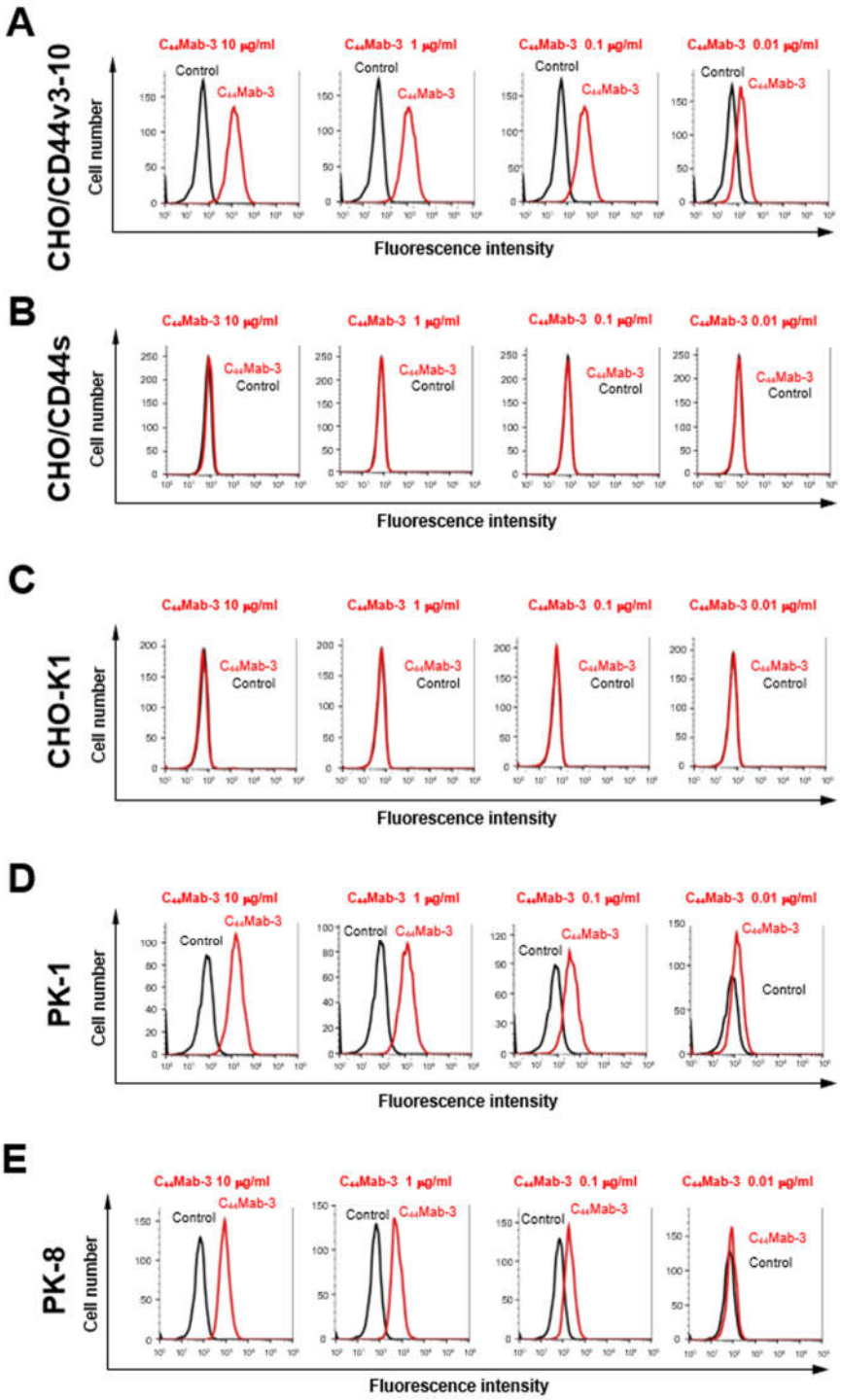

Figure 2. Flow cytometry using C44Mab-3 against CD44-expressing cells. CHO/CD44v3–10 (**A**), CHO/CD44s (**B**), CHO-K1 (**C**), PK-1 (**D**), and PK-8 (**E**) cells were treated with 0.01-10 μg/mL of C44Mab-3, followed by treatment with Alexa Fluor 488-conjugated anti-mouse IgG (Red line). The black line represents the negative control (blocking buffer).

Preprints (www.preprints.org) | NOT PEER-REVIEWED | Posted: 31 January 2023 doi:10.20944/preprints202301.0581.v1

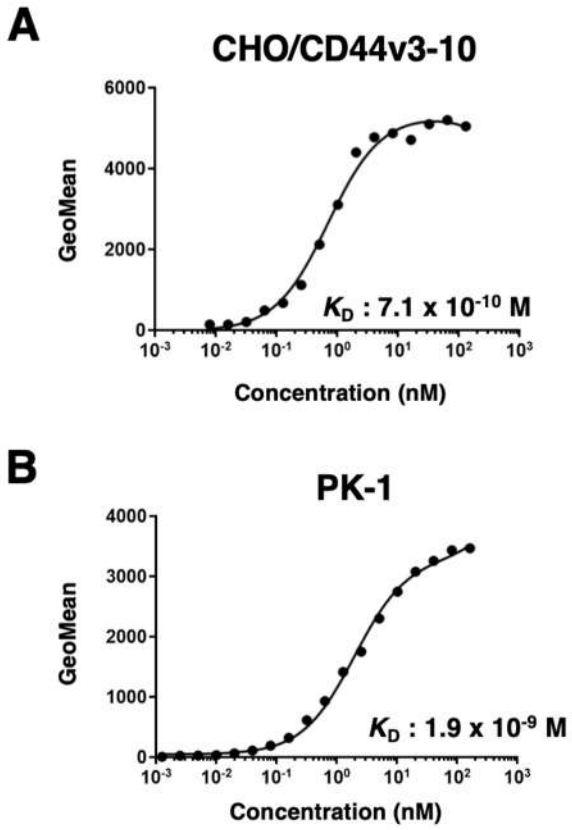

Figure 3. The binding affinity of C44Mab-3 to CD44-expressing cells. CHO/CD44v3–10 (**A**) and PK-1 (**B**) cells were suspended in 100 μL of serially diluted C44Mab-3 (0.0006–10 μg/mL). The cells were incubated with Alexa Fluor 488-conjugated anti-mouse IgG. The apparent dissociation constant (*K*D) was measured by GraphPad PRISM 8 using the fluorescence data.

3.3. Western Blot Analysis

We next performed western blot analysis to examine the sensitivity of C44Mab-3. Total cell lysates of CHO-K1, CHO/CD44s, CHO/CD44v3–10, PK-1, and PK-8 were analyzed. As shown in Figure 4A, an anti-pan-CD44 mAb, C44Mab-46, recognized the lysates from both CHO/CD44s (~75 kDa) and CHO/CD44v3–10 (> 180 kDa). C44Mab-3 detected CD44v3–10 as a more than 180-kDa bands. Furthermore, C44Mab-3 detected endonenous CD44v5-containing CD44v in PK-1 and PK-8 cells. However, C44Mab-3 did not detect any bands from lysates of CHO/CD44s and CHO-K1 cells (Figure 4B). An anti-PA16 tag mAb (NZ-1) recognized the lysates from both CHO/CD44s (~75 kDa) and CHO/CD44v3–10 (> 180 kDa) (Figure 4C). These results indicated that C44Mab-3 specifically detects exogenous CD44v3–10 and endogenous CD44v5-containing CD44v.

Preprints (www.preprints.org) | NOT PEER-REVIEWED | Posted: 31 January 2023 doi:10.20944/preprints202301.0581.v1

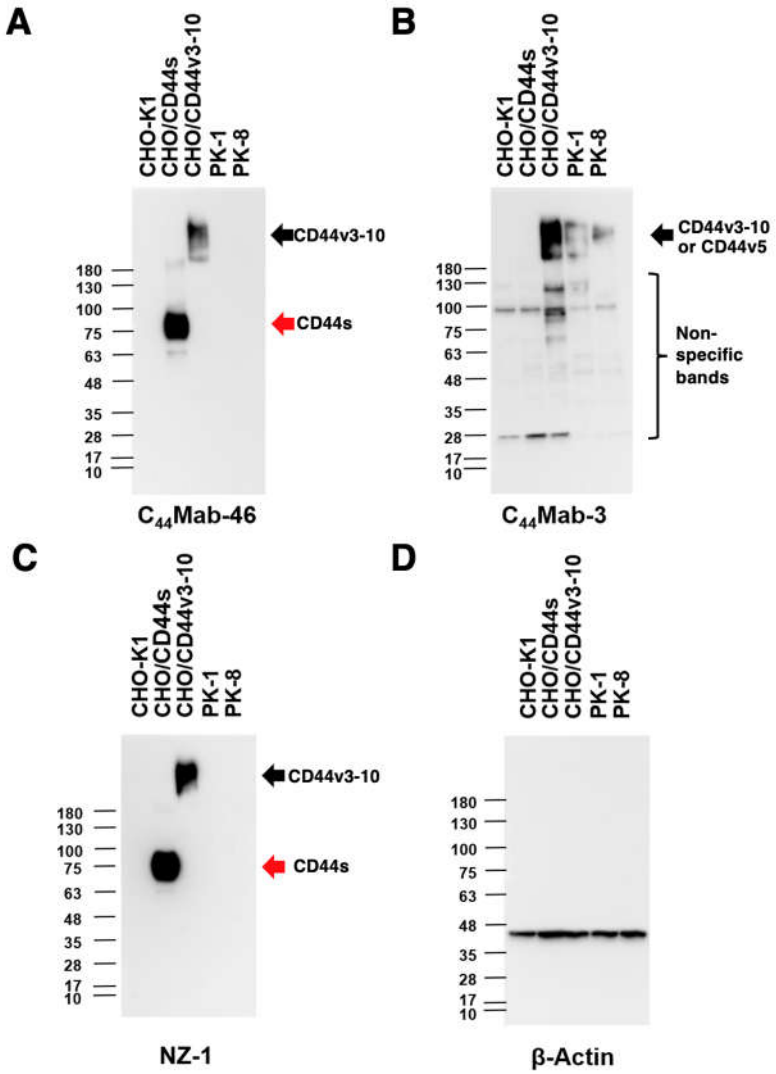

Figure 4. Western blot analysis using C44Mab-3. The cell lysates of CHO-K1, CHO/CD44s, CHO/CD44v3–10, PK-1, and PK-8 (10 μg) were separated and transferred onto polyvinylidene fluoride membranes. The membranes were incubated with 10 μg/mL of C44Mab-46 (**A**), 10 μg/mL of C44Mab-3 (**B**), 0.5 μg/mL of anti-PA16 tag mAb (NZ-1) (**C**), and 1 μg/mL of an anti-β-actin mAb (**D**). Then, the membranes were incubated with anti-mouse immunoglobulins conjugated with peroxidase for C44Mab-46, C44Mab-3, and anti-β-actin. The anti-rat immunoglobulins conjugated with peroxidase was used for NZ-1. The red arrows indicate the CD44s (~75 kDa). The black arrows indicate the CD44v3–10 or CD44v5 (>180 kDa).

3.4. Immunohistochemistry using C44Mab-3 against Tumor Tissues

We next examined whether C44Mab-3 is applicable to immunohistochemistry in FFPE sections. We first examined the reactivity of C44Mab-3 and C44Mab-46 in an oral SCC tissue. As shown in supplemental Figure S2, C44Mab-3 exhibited a clear membranous staining, and could clearly distinguish tumor cells from stromal tissues. In contrast, C44Mab-46 stained the both. We then investigated the reactivity of C44Mab-3 and C44Mab-46 in pancreatic carcinoma tissue arrays. Although we performed the antigen retrieval using citrate buffer (pH 6.0) for pancreatic carcinoma tissue arrays in the same way with an oral SCC tissue, weak staining was observed (data not shown). We next used EnVision FLEX Target Retrieval Solution High pH for antigen retrieval procedure, C44Mab-3 showed the clear membranous staining in pancreatic carcinoma cells with relatively larger cytoplasm (Figure 5A). C44Mab-46 also stained the same type of pancreatic carcinoma cells (Figure 5B). The staining intensity of C44Mab-3 was much stronger than that of C44Mab-46 (Figure 5A, 5B). Furthermore, diffusely spread tumor cells in stroma were stained by both C44Mab-3

Preprints (www.preprints.org) | NOT PEER-REVIEWED | Posted: 31 January 2023 doi:10.20944/preprints202301.0581.v1

and C44Mab-46 (Figure 5C and D). In contrast, both C44Mab-3 and C44Mab-46 never stained the typical ductal structure of PDAC (Figure 5E and F). In addition, stromal staining by C44Mab-46 was observed in several tissues (Figure 5F). Importantly, normal pancreatic epithelial cells were never stained by C44Mab-3 (Figure 5G). Similar staining pattern was also observed in another tissue array (supplementary Figure S3). We summarized the data of immunohistochemical analyses in Table 1; C44Mab-3 stained 8 out of 20 cases (40 %) (PA484, Figure 5), and 2 out of 6 cases (33 %) (PA241c, supplementary Figure S3) in pancreatic carcinomas. These results indicated that C44Mab-3 is useful for immunohistochemistry of FFPE tumor sections, and could recognize a specific type of pancreatic carcinomas.

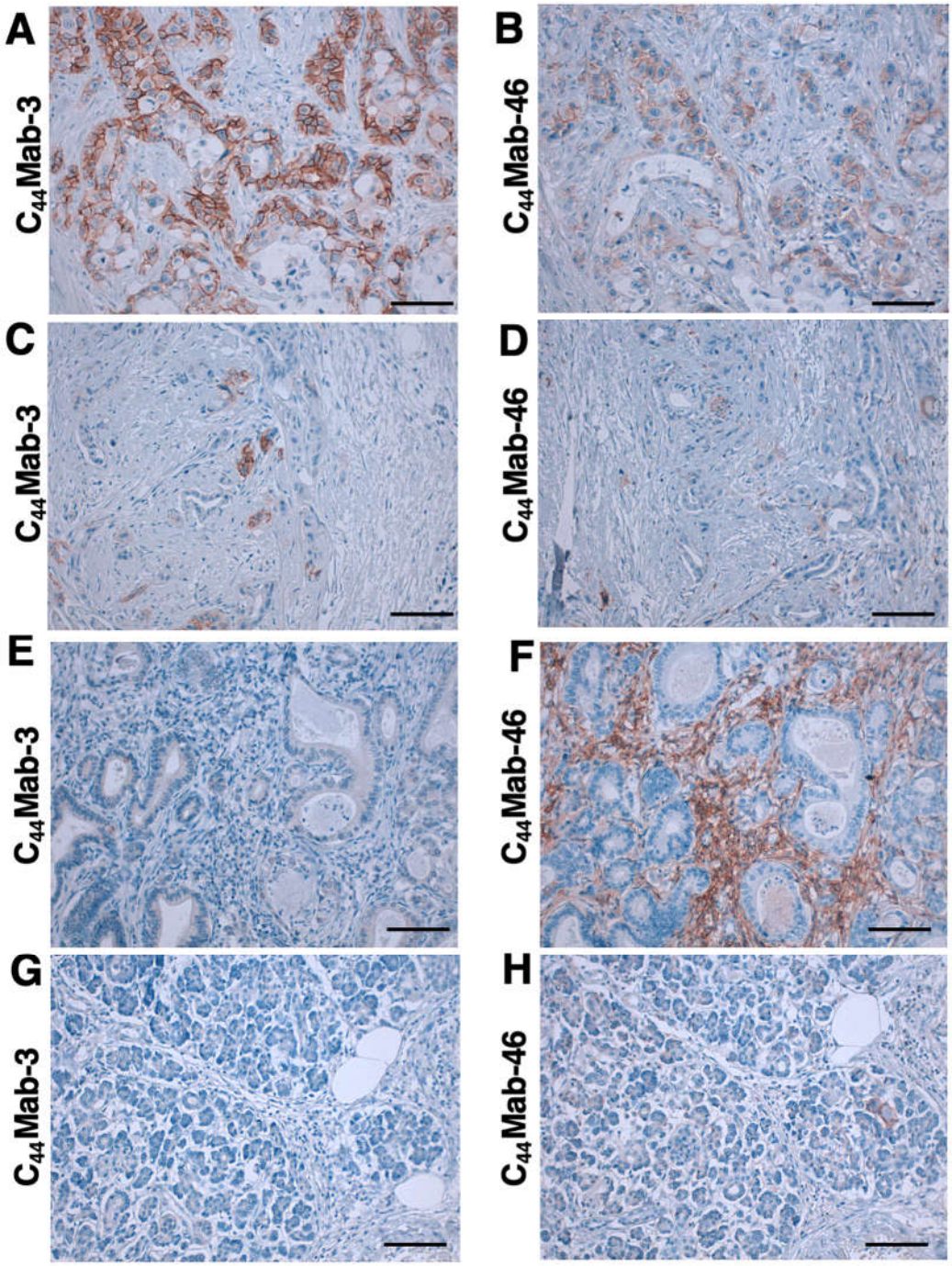

Figure 5. Immunohistochemical analysis using C44Mab-3 and C44Mab-46 against pancreatic adenocarcinomas and normal pancreatic tissues. After antigen retrieval, serial sections of pancreatic carcinoma tissue arrays (Catalog number: PA484) were incubated with 1 μg/mL of C44Mab-3 or C44Mab-46 followed by treatment with the Envision+ kit. The color was developed using 3,3′-

Preprints (www.preprints.org) | NOT PEER-REVIEWED | Posted: 31 January 2023 doi:10.20944/preprints202301.0581.v1

diaminobenzidine tetrahydrochloride (DAB), and the sections were counterstained with hematoxylin. Scale bar = 100 μm. (**A–F**) pancreatic adenocarcinomas; (**G, H**) normal pancreas tissues.

Table 1. Immunohistochemical analysis using C$_{44}$Mab-3 and C$_{44}$Mab-46 against pancreatic carcinoma tissue arrays.

Tissue array	Age	Sex	Organ	Pathology diagnosis	TNM	Grade	Stage	Type	C$_{44}$Mab-3
PA241c	66	F	Pancreas	Adenocarcinoma	T2N0M0	1	I	malignant	+
	66	F	Pancreas	Adjacent normal pancreas tissue					–
	54	F	Pancreas	Adenocarcinoma	T3N0M0	2	II	malignant	–
	54	F	Pancreas	Adjacent normal pancreas tissue					–
	44	M	Pancreas	Adenocarcinoma	T3N0M0	2	II	malignant	–
	44	M	Pancreas	Adjacent normal pancreas tissue					–
	59	M	Pancreas	Adenocarcinoma	T2N0M0	3	I	malignant	–
	59	M	Pancreas	Adjacent normal pancreas tissue					–
	63	F	Pancreas	Adenocarcinoma	T2N0M0	3	I	malignant	+
	63	F	Pancreas	Adjacent normal pancreas tissue					–
	53	F	Pancreas	Adenocarcinoma	T3N0M0	3	II	malignant	–
	53	F	Pancreas	Adjacent normal pancreas tissue					–
PA484	35	M	Pancreas	Normal pancreas tissue	-	-	-	normal	–
	38	F	Pancreas	Normal pancreas tissue	-	-	-	normal	–
	38	M	Pancreas	Normal pancreas tissue	-	-	-	normal	–
	60	M	Pancreas	Adenocarcinoma	T3N0M0	2	II	malignant	–
	68	F	Pancreas	Adenocarcinoma	T2N0M0	2	I	malignant	+
	54	F	Pancreas	Adenocarcinoma	T3N0M0	2	II	malignant	–
	42	F	Pancreas	Adenocarcinoma	T3N0M0	2	II	malignant	–
	65	M	Pancreas	Adenocarcinoma	T3N0M0	2	II	malignant	–
	75	F	Pancreas	Adenocarcinoma	T3N0M1	2	IV	malignant	–
	57	M	Pancreas	Adenocarcinoma	T3N0M0	3	II	malignant	+
	44	M	Pancreas	Adenocarcinoma	T3N0M0	3	II	malignant	–
	47	M	Pancreas	Adenocarcinoma	T3N0M0	-	II	malignant	–
	41	M	Pancreas	Adenocarcinoma	T4N1M0	2	III	malignant	–
	64	F	Pancreas	Adenocarcinoma	T3N0M0	2	II	malignant	–
	58	F	Pancreas	Adenocarcinoma	T3N0M0	3	II	malignant	–
	47	F	Pancreas	Adenocarcinoma	T3N1M0	3	III	malignant	+
	78	M	Pancreas	Adenocarcinoma	T2N0M0	3	I	malignant	+
	49	M	Pancreas	Adenocarcinoma	T3N0M0	2	II	malignant	+
	53	F	Pancreas	Adenocarcinoma	T3N0M0	3	II	malignant	+
	60	M	Pancreas	Adenocarcinoma	T2N0M0	3	I	malignant	+
	57	F	Pancreas	Adenocarcinoma	T2N0M0	3	I	malignant	–
	61	M	Pancreas	Mucinous adenocarcinoma	T3N0M1	2	IV	malignant	–
	69	M	Pancreas	Undifferentiated carcinoma	T2N0M0	-	I	malignant	+

Preprints (www.preprints.org) | NOT PEER-REVIEWED | Posted: 31 January 2023 doi:10.20944/preprints202301.0581.v1

4. Discussion

Pancreatic cancer is the third leading cause of cancer death in United States [1]. PDAC is the most common type of pancreatic cancer, and exhibits the extremely poor prognosis with a 5-year survival rate of approximately 10% [49]. Advances in therapy have only achieved incremental improvements in overall outcome, but can provide notable benefit for undefined subgroups of patients. PDACs are heterogenous neoplasms with various histology [4] and heterogenous molecular landscapes [5]. Therefore, the identification of early diagnostic markers and therapeutic targets in each group has been desired. In this study, we developed C$_{44}$Mab-3 using the CBIS method (Figure 1), and determined its epitope as variant 5-encoded region of CD44 (supplementary Table S1). Then, we showed the usefulness of C$_{44}$Mab-3 for multiple applications, including flow cytometry (Figure 2 and 3), western blotting (Figure 4), and immunohistochemistry of PDAC (Figure 5).

An anti-CD44v5 mAb (clone VFF-8) was previously developed and mainly used for the immunohistochemical analyses of tumors [50]. The epitope of VFF-8 was determined as IHHEHHEEEETPHSTST in v5-encoded region by ELISA [51]. As shown in supplementary Table S1, C$_{44}$Mab-3 recognized both CD44p311–330 and CD44p321–340 peptides, which commonly possess HPPLIHHEHH sequence. The epitope of C$_{44}$Mab-3 partially shares that of VFF-8. Further investigation of the detailed epitope mapping is required. In addition, CD44 is known to be heavily glycosylated [52], and the glycosylation pattern is thought to depend on the host cells. Since the epitope of C$_{44}$Mab-3 never contains serine or threonine, the recognition of C$_{44}$Mab-3 is thought to be independent of the glycosylation.

Immunohistochemistry using VFF-8 and conventional RT-PCR analyses were performed against PDAC [50]. VFF-8 recognized PDAC, but not normal pancreas. Furthermore, RT-PCR analysis revealed that the exon v5 appeared in the chain containing at least v4–10 in 80% of PDAC and the cell lines tested. The authors discussed that one of the major differences between normal and PDAC was the linkage of CD44v5 to the CD44v6-containing chain [50]. Our immunohistochemical analysis also support the finding (Figure 5A, C, and G). Furthermore, we found that C$_{44}$Mab-3 could detect atypical type of PDAC, including metaplastic and diffusely invaded tumor cells (Figure 5A and C). In contrast, C$_{44}$Mab-3 never stained a typical ductal structure of PDAC (Figure 5E) and normal pancreatic epithelial cells (Figure 5G). In addition to conventional PDAC, the World Health Organization classified nine histological subtypes of PDAC, which further highlight the morphologic heterogeneity of PDAC [4]. It is worthwhile to investigate whether CD44v5 is expressed in a specific subtype of PDAC in the future study.

Large scale genomic analyses of PDACs defined 4 subtypes: (1) squamous; (2) pancreatic progenitor; (3) immunogenic; and (4) ADEX, that correlate with histopathological characteristics [5]. Among them, squamous subtype is characterized as enriched for *TP53* and *KDM6A* mutations, upregulation of the ΔNp63 transcriptional network, hypermethylation of pancreatic endodermal determinant genes and have a poor prognosis [5]. ΔNp63 is known as a marker of basal cells of stratified epithelium and SCC [53], and also reported to regulate HA metabolism and signaling [54]. Especially, ΔNp63 directly regulates the expression of CD44 through p63-binding sites, which are located in the promoter region and in the first intron of CD44 gene, respectively [54]. Therefore, CD44 transcription could be upregulated in ΔNp63-positive PDAC. However, the mechanism of the variant 5 inclusion during alternative splicing remains to be determined.

Clinical trials of anti-pan CD44 and variant-specific CD44 mAbs have been conducted [55]. An anti-pan CD44 mAb, RG7356, was well tolerated in patients with advanced CD44-positive solid tumors. However, the study was terminated because of no evidence of a clinical and dose-response relationship with RG7356 [56]. A clinical trial of humanized anti-CD44v6 mAb bivatuzumab−mertansine drug conjugate was conducted. However, it failed due to the severe skin toxicities [57,58]. The efficient accumulation of mertansine was most likely responsible for the high toxicity [57,58]. Although CD44v5 is never detected in normal pancreatic epithelium by C$_{44}$Mab-3 (this study) and VFF-8 [50],

Preprints (www.preprints.org) | NOT PEER-REVIEWED | Posted: 31 January 2023 doi:10.20944/preprints202301.0581.v1

CD44v5 could be detected in normal lung, skin, gastric, and bladder epithelium by VFF-8 [51]. For the development of therapeutic use of C44Mab-3, further investigations are required to reduce the toxicity to above tissues.

Our group converted mouse IgG_1 subclass of mAbs into a IgG_{2a}, and produced a defucosylated mAbs using fucosyltransferases 8-deficient CHO-K1 cells. The defucosylated IgG_{2a} mAbs showed potent antibody-dependent cellular cytotoxicity *in vitro*, and suppressed the tumor xenograft growth [27,59-65]. Therefore, the production of a class-switched and defucosylated version of C44Mab-3 is required to evaluate the antitumor activity *in vivo*.

Supplementary Materials: Table S1, The determination of the binding epitope of C44Mab-3 by ELISA. Figure S1, Recognition of CHO/CD44s and CHO/CD44v3–10 by C44Mab-46 by flow cytometry. Figure S2, Immunohistochemical analysis using C44Mab-3 and C44Mab-46 against oral squamous cell carcinoma tissues. Figure S3, Immunohistochemical analysis using C44Mab-3 and C44Mab-46 against pancreatic adenocarcinomas and normal pancreatic tissues.

Author Contributions: Y.Kudo, H.S., and T.T. performed the experiments. M.K.K. and Y.Kato designed the experiments. H.S. and Y.Kudo analyzed the data. Y.Kudo, H.S. and Y.Kato wrote the manuscript. All authors have read and agreed to the manuscript.

Funding: This research was supported in part by Japan Agency for Medical Research and Development (AMED) under Grant Numbers: JP22ama121008 (to Y.K.), JP22am0401013 (to Y.K.), JP22bm1004001 (to Y.K.), JP22ck0106730 (to Y.K.), and JP21am0101078 (to Y.K.), and by the Japan Society for the Promotion of Science (JSPS) Grants-in-Aid for Scientific Research (KAKENHI) grant nos. 21K20789 (to T.T.), 22K06995 (to H.S.), 22K07168 (to M.K.K.), and 22K07224 (to Y.K.).

Institutional Review Board Statement: The animal study protocol was approved by the Animal Care and Use Committee of Tohoku University (Permit number: 2019NiA-001) for studies involving animals.

Data Availability Statement: The data presented in this study are available in the article and supplementary material.

Conflicts of Interest: The authors have no conflicts of interest to declare.

References

1. Siegel, R.L.; Miller, K.D.; Fuchs, H.E.; Jemal, A. Cancer statistics, 2022. *CA Cancer J Clin* **2022**, *72*, 7-33, doi:10.3322/caac.21708.
2. Jones, S.; Zhang, X.; Parsons, D.W.; Lin, J.C.; Leary, R.J.; Angenendt, P.; Mankoo, P.; Carter, H.; Kamiyama, H.; Jimeno, A.; et al. Core signaling pathways in human pancreatic cancers revealed by global genomic analyses. *Science* **2008**, *321*, 1801-1806, doi:10.1126/science.1164368.
3. Waddell, N.; Pajic, M.; Patch, A.M.; Chang, D.K.; Kassahn, K.S.; Bailey, P.; Johns, A.L.; Miller, D.; Nones, K.; Quek, K.; et al. Whole genomes redefine the mutational landscape of pancreatic cancer. *Nature* **2015**, *518*, 495-501, doi:10.1038/nature14169.
4. Taherian, M.; Wang, H.; Wang, H. Pancreatic Ductal Adenocarcinoma: Molecular Pathology and Predictive Biomarkers. *Cells* **2022**, *11*, doi:10.3390/cells11193068.
5. Bailey, P.; Chang, D.K.; Nones, K.; Johns, A.L.; Patch, A.M.; Gingras, M.C.; Miller, D.K.; Christ, A.N.; Bruxner, T.J.; Quinn, M.C.; et al. Genomic analyses identify molecular subtypes of pancreatic cancer. *Nature* **2016**, *531*, 47-52, doi:10.1038/nature16965.
6. Puccini, A.; Seeber, A.; Berger, M.D. Biomarkers in Metastatic Colorectal Cancer: Status Quo and Future Perspective. *Cancers (Basel)* **2022**, *14*, doi:10.3390/cancers14194828.
7. Zöller, M. CD44: can a cancer-initiating cell profit from an abundantly expressed molecule? *Nat Rev Cancer* **2011**, *11*, 254-267, doi:10.1038/nrc3023.
8. Abbasian, M.; Mousavi, E.; Arab-Bafrani, Z.; Sahebkar, A. The most reliable surface marker for the identification of colorectal cancer stem-like cells: A systematic review and meta-analysis. *J Cell Physiol* **2019**, *234*, 8192-8202, doi:10.1002/jcp.27619.
9. Fox, S.B.; Fawcett, J.; Jackson, D.G.; Collins, I.; Gatter, K.C.; Harris, A.L.; Gearing, A.; Simmons, D.L. Normal human tissues, in addition to some tumors, express multiple different CD44 isoforms. *Cancer Res* **1994**, *54*, 4539-4546.
10. Yan, Y.; Zuo, X.; Wei, D. Concise Review: Emerging Role of CD44 in Cancer Stem Cells: A Promising Biomarker and Therapeutic Target. *Stem Cells Transl Med* **2015**, *4*, 1033-1043, doi:10.5966/sctm.2015-0048.
11. Chen, C.; Zhao, S.; Karnad, A.; Freeman, J.W. The biology and role of CD44 in cancer progression: therapeutic implications. *J Hematol Oncol* **2018**, *11*, 64, doi:10.1186/s13045-018-0605-5.
12. Slevin, M.; Krupinski, J.; Gaffney, J.; Matou, S.; West, D.; Delisser, H.; Savani, R.C.; Kumar, S. Hyaluronan-mediated angiogenesis in vascular disease: uncovering RHAMM and CD44 receptor signaling pathways. *Matrix Biol* **2007**, *26*, 58-68, doi:10.1016/j.matbio.2006.08.261.

13. Uchino, M.; Kojima, H.; Wada, K.; Imada, M.; Onoda, F.; Satofuka, H.; Utsugi, T.; Murakami, Y. Nuclear beta-catenin and CD44 upregulation characterize invasive cell populations in non-aggressive MCF-7 breast cancer cells. *BMC Cancer* **2010**, *10*, 414, doi:10.1186/1471-2407-10-414.
14. Naor, D.; Wallach-Dayan, S.B.; Zahalka, M.A.; Sionov, R.V. Involvement of CD44, a molecule with a thousand faces, in cancer dissemination. *Semin Cancer Biol* **2008**, *18*, 260-267, doi:10.1016/j.semcancer.2008.03.015.
15. Günthert, U.; Hofmann, M.; Rudy, W.; Reber, S.; Zöller, M.; Haussmann, I.; Matzku, S.; Wenzel, A.; Ponta, H.; Herrlich, P. A new variant of glycoprotein CD44 confers metastatic potential to rat carcinoma cells. *Cell* **1991**, *65*, 13-24, doi:10.1016/0092-8674(91)90403-l.
16. Guo, Q.; Yang, C.; Gao, F. The state of CD44 activation in cancer progression and therapeutic targeting. *Febs j* **2021**, doi:10.1111/febs.16179.
17. Hassn Mesrati, M.; Syafruddin, S.E.; Mohtar, M.A.; Syahir, A. CD44: A Multifunctional Mediator of Cancer Progression. *Biomolecules* **2021**, *11*, doi:10.3390/biom11121850.
18. Morath, I.; Hartmann, T.N.; Orian-Rousseau, V. CD44: More than a mere stem cell marker. *Int J Biochem Cell Biol* **2016**, *81*, 166-173, doi:10.1016/j.biocel.2016.09.009.
19. Bennett, K.L.; Jackson, D.G.; Simon, J.C.; Tanczos, E.; Peach, R.; Modrell, B.; Stamenkovic, I.; Plowman, G.; Aruffo, A. CD44 isoforms containing exon V3 are responsible for the presentation of heparin-binding growth factor. *J Cell Biol* **1995**, *128*, 687-698, doi:10.1083/jcb.128.4.687.
20. Orian-Rousseau, V.; Chen, L.; Sleeman, J.P.; Herrlich, P.; Ponta, H. CD44 is required for two consecutive steps in HGF/c-Met signaling. *Genes Dev* **2002**, *16*, 3074-3086, doi:10.1101/gad.242602.
21. Ishimoto, T.; Nagano, O.; Yae, T.; Tamada, M.; Motohara, T.; Oshima, H.; Oshima, M.; Ikeda, T.; Asaba, R.; Yagi, H.; et al. CD44 variant regulates redox status in cancer cells by stabilizing the xCT subunit of system xc(-) and thereby promotes tumor growth. *Cancer Cell* **2011**, *19*, 387-400, doi:10.1016/j.ccr.2011.01.038.
22. Yamada, S.; Itai, S.; Nakamura, T.; Yanaka, M.; Kaneko, M.K.; Kato, Y. Detection of high CD44 expression in oral cancers using the novel monoclonal antibody, C(44)Mab-5. *Biochem Biophys Rep* **2018**, *14*, 64-68, doi:10.1016/j.bbrep.2018.03.007.
23. Goto, N.; Suzuki, H.; Tanaka, T.; Asano, T.; Kaneko, M.K.; Kato, Y. Development of a Novel Anti-CD44 Monoclonal Antibody for Multiple Applications against Esophageal Squamous Cell Carcinomas. *Int J Mol Sci* **2022**, *23*, doi:10.3390/ijms23105535.
24. Takei, J.; Asano, T.; Suzuki, H.; Kaneko, M.K.; Kato, Y. Epitope Mapping of the Anti-CD44 Monoclonal Antibody (C44Mab-46) Using Alanine-Scanning Mutagenesis and Surface Plasmon Resonance. *Monoclon Antib Immunodiagn Immunother* **2021**, *40*, 219-226, doi:10.1089/mab.2021.0028.
25. Asano, T.; Kaneko, M.K.; Takei, J.; Tateyama, N.; Kato, Y. Epitope Mapping of the Anti-CD44 Monoclonal Antibody (C44Mab-46) Using the REMAP Method. *Monoclon Antib Immunodiagn Immunother* **2021**, *40*, 156-161, doi:10.1089/mab.2021.0012.
26. Asano, T.; Kaneko, M.K.; Kato, Y. Development of a Novel Epitope Mapping System: RIEDL Insertion for Epitope Mapping Method. *Monoclon Antib Immunodiagn Immunother* **2021**, *40*, 162-167, doi:10.1089/mab.2021.0023.
27. Takei, J.; Kaneko, M.K.; Ohishi, T.; Hosono, H.; Nakamura, T.; Yanaka, M.; Sano, M.; Asano, T.; Sayama, Y.; Kawada, M.; et al. A defucosylated antiCD44 monoclonal antibody 5mG2af exerts antitumor effects in mouse xenograft models of oral squamous cell carcinoma. *Oncol Rep* **2020**, *44*, 1949-1960, doi:10.3892/or.2020.7735.
28. Kato, Y.; Yamada, S.; Furusawa, Y.; Itai, S.; Nakamura, T.; Yanaka, M.; Sano, M.; Harada, H.; Fukui, M.; Kaneko, M.K. PMab-213: A Monoclonal Antibody for Immunohistochemical Analysis Against Pig Podoplanin. *Monoclon Antib Immunodiagn Immunother* **2019**, *38*, 18-24, doi:10.1089/mab.2018.0048.
29. Furusawa, Y.; Yamada, S.; Itai, S.; Sano, M.; Nakamura, T.; Yanaka, M.; Fukui, M.; Harada, H.; Mizuno, T.; Sakai, Y.; et al. PMab-210: A Monoclonal Antibody Against Pig Podoplanin. *Monoclon Antib Immunodiagn Immunother* **2019**, *38*, 30-36, doi:10.1089/mab.2018.0038.
30. Furusawa, Y.; Yamada, S.; Itai, S.; Nakamura, T.; Yanaka, M.; Sano, M.; Harada, H.; Fukui, M.; Kaneko, M.K.; Kato, Y. PMab-219: A monoclonal antibody for the immunohistochemical analysis of horse podoplanin. *Biochem Biophys Rep* **2019**, *18*, 100616, doi:10.1016/j.bbrep.2019.01.009.
31. Furusawa, Y.; Yamada, S.; Itai, S.; Nakamura, T.; Takei, J.; Sano, M.; Harada, H.; Fukui, M.; Kaneko, M.K.; Kato, Y. Establishment of a monoclonal antibody PMab-233 for immunohistochemical analysis against Tasmanian devil podoplanin. *Biochem Biophys Rep* **2019**, *18*, 100631, doi:10.1016/j.bbrep.2019.100631.
32. Kato, Y.; Kaneko, M.K.; Kuno, A.; Uchiyama, N.; Amano, K.; Chiba, Y.; Hasegawa, Y.; Hirabayashi, J.; Narimatsu, H.; Mishima, K.; et al. Inhibition of tumor cell-induced platelet aggregation using a novel anti-podoplanin antibody reacting with its platelet-aggregation-stimulating domain. *Biochem Biophys Res Commun* **2006**, *349*, 1301-1307, doi:10.1016/j.bbrc.2006.08.171.
33. Chalise, L.; Kato, A.; Ohno, M.; Maeda, S.; Yamamichi, A.; Kuramitsu, S.; Shiina, S.; Takahashi, H.; Ozone, S.; Yamaguchi, J.; et al. Efficacy of cancer-specific anti-podoplanin CAR-T cells and oncolytic herpes virus G47Delta combination therapy against glioblastoma. *Mol Ther Oncolytics* **2022**, *26*, 265-274, doi:10.1016/j.omto.2022.07.006.
34. Ishikawa, A.; Waseda, M.; Ishii, T.; Kaneko, M.K.; Kato, Y.; Kaneko, S. Improved anti-solid tumor response by humanized anti-podoplanin chimeric antigen receptor transduced human cytotoxic T cells in an animal model. *Genes Cells* **2022**, *27*, 549-558, doi:10.1111/gtc.12972.
35. Tamura-Sakaguchi, R.; Aruga, R.; Hirose, M.; Ekimoto, T.; Miyake, T.; Hizukuri, Y.; Oi, R.; Kaneko, M.K.; Kato, Y.; Akiyama, Y.; et al. Moving toward generalizable NZ-1 labeling for 3D structure determination with optimized epitope-tag insertion. *Acta Crystallogr D Struct Biol* **2021**, *77*, 645-662, doi:10.1107/S2059798321002527.

Preprints (www.preprints.org) | NOT PEER-REVIEWED | Posted: 31 January 2023 doi:10.20944/preprints202301.0581.v1

36. Kaneko, M.K.; Ohishi, T.; Nakamura, T.; Inoue, H.; Takei, J.; Sano, M.; Asano, T.; Sayama, Y.; Hosono, H.; Suzuki, H.; et al. Development of Core-Fucose-Deficient Humanized and Chimeric Anti-Human Podoplanin Antibodies. *Monoclon Antib Immunodiagn Immunother* **2020**, *39*, 167-174, doi:10.1089/mab.2020.0019.
37. Fujii, Y.; Matsunaga, Y.; Arimori, T.; Kitago, Y.; Ogasawara, S.; Kaneko, M.K.; Kato, Y.; Takagi, J. Tailored placement of a turn-forming PA tag into the structured domain of a protein to probe its conformational state. *J Cell Sci* **2016**, *129*, 1512-1522, doi:10.1242/jcs.176685.
38. Abe, S.; Kaneko, M.K.; Tsuchihashi, Y.; Izumi, T.; Ogasawara, S.; Okada, N.; Sato, C.; Tobiume, M.; Otsuka, K.; Miyamoto, L.; et al. Antitumor effect of novel anti-podoplanin antibody NZ-12 against malignant pleural mesothelioma in an orthotopic xenograft model. *Cancer Sci* **2016**, *107*, 1198-1205, doi:10.1111/cas.12985.
39. Kaneko, M.K.; Abe, S.; Ogasawara, S.; Fujii, Y.; Yamada, S.; Murata, T.; Uchida, H.; Tahara, H.; Nishioka, Y.; Kato, Y. Chimeric Anti-Human Podoplanin Antibody NZ-12 of Lambda Light Chain Exerts Higher Antibody-Dependent Cellular Cytotoxicity and Complement-Dependent Cytotoxicity Compared with NZ-8 of Kappa Light Chain. *Monoclon Antib Immunodiagn Immunother* **2017**, *36*, 25-29, doi:10.1089/mab.2016.0047.
40. Ito, A.; Ohta, M.; Kato, Y.; Inada, S.; Kato, T.; Nakata, S.; Yatabe, Y.; Goto, M.; Kaneda, N.; Kurita, K.; et al. A Real-Time Near-Infrared Fluorescence Imaging Method for the Detection of Oral Cancers in Mice Using an Indocyanine Green-Labeled Podoplanin Antibody. *Technol Cancer Res Treat* **2018**, *17*, 1533033818767936, doi:10.1177/1533033818767936.
41. Tamura, R.; Oi, R.; Akashi, S.; Kaneko, M.K.; Kato, Y.; Nogi, T. Application of the NZ-1 Fab as a crystallization chaperone for PA tag-inserted target proteins. *Protein Sci* **2019**, *28*, 823-836, doi:10.1002/pro.3580.
42. Shiina, S.; Ohno, M.; Ohka, F.; Kuramitsu, S.; Yamamichi, A.; Kato, A.; Motomura, K.; Tanahashi, K.; Yamamoto, T.; Watanabe, R.; et al. CAR T Cells Targeting Podoplanin Reduce Orthotopic Glioblastomas in Mouse Brains. *Cancer Immunol Res* **2016**, *4*, 259-268, doi:10.1158/2326-6066.CIR-15-0060.
43. Kuwata, T.; Yoneda, K.; Mori, M.; Kanayama, M.; Kuroda, K.; Kaneko, M.K.; Kato, Y.; Tanaka, F. Detection of Circulating Tumor Cells (CTCs) in Malignant Pleural Mesothelioma (MPM) with the "Universal" CTC-Chip and An Anti-Podoplanin Antibody NZ-1.2. *Cells* **2020**, *9*, doi:10.3390/cells9040888.
44. Nishinaga, Y.; Sato, K.; Yasui, H.; Taki, S.; Takahashi, K.; Shimizu, M.; Endo, R.; Koike, C.; Kuramoto, N.; Nakamura, S.; et al. Targeted Phototherapy for Malignant Pleural Mesothelioma: Near-Infrared Photoimmunotherapy Targeting Podoplanin. *Cells* **2020**, *9*, doi:10.3390/cells9041019.
45. Fujii, Y.; Kaneko, M.; Neyazaki, M.; Nogi, T.; Kato, Y.; Takagi, J. PA tag: a versatile protein tagging system using a super high affinity antibody against a dodecapeptide derived from human podoplanin. *Protein Expr Purif* **2014**, *95*, 240-247, doi:10.1016/j.pep.2014.01.009.
46. Kato, Y.; Kaneko, M.K.; Kunita, A.; Ito, H.; Kameyama, A.; Ogasawara, S.; Matsuura, N.; Hasegawa, Y.; Suzuki-Inoue, K.; Inoue, O.; et al. Molecular analysis of the pathophysiological binding of the platelet aggregation-inducing factor podoplanin to the C-type lectin-like receptor CLEC-2. *Cancer Sci* **2008**, *99*, 54-61, doi:10.1111/j.1349-7006.2007.00634.x.
47. Kato, Y.; Vaidyanathan, G.; Kaneko, M.K.; Mishima, K.; Srivastava, N.; Chandramohan, V.; Pegram, C.; Keir, S.T.; Kuan, C.T.; Bigner, D.D.; et al. Evaluation of anti-podoplanin rat monoclonal antibody NZ-1 for targeting malignant gliomas. *Nucl Med Biol* **2010**, *37*, 785-794, doi:10.1016/j.nucmedbio.2010.03.010.
48. Itai, S.; Ohishi, T.; Kaneko, M.K.; Yamada, S.; Abe, S.; Nakamura, T.; Yanaka, M.; Chang, Y.W.; Ohba, S.I.; Nishioka, Y.; et al. Anti-podocalyxin antibody exerts antitumor effects via antibody-dependent cellular cytotoxicity in mouse xenograft models of oral squamous cell carcinoma. *Oncotarget* **2018**, *9*, 22480-22497, doi:10.18632/oncotarget.25132.
49. Kamisawa, T.; Wood, L.D.; Itoi, T.; Takaori, K. Pancreatic cancer. *Lancet* **2016**, *388*, 73-85, doi:10.1016/s0140-6736(16)00141-0.
50. Gansauge, F.; Gansauge, S.; Zobywalski, A.; Scharnweber, C.; Link, K.H.; Nussler, A.K.; Beger, H.G. Differential expression of CD44 splice variants in human pancreatic adenocarcinoma and in normal pancreas. *Cancer Res* **1995**, *55*, 5499-5503.
51. Heider, K.H.; Mulder, J.W.; Ostermann, E.; Susani, S.; Patzelt, E.; Pals, S.T.; Adolf, G.R. Splice variants of the cell surface glycoprotein CD44 associated with metastatic tumour cells are expressed in normal tissues of humans and cynomolgus monkeys. *Eur J Cancer* **1995**, *31a*, 2385-2391, doi:10.1016/0959-8049(95)00420-3.
52. Mereiter, S.; Martins Á, M.; Gomes, C.; Balmaña, M.; Macedo, J.A.; Polom, K.; Roviello, F.; Magalhães, A.; Reis, C.A. O-glycan truncation enhances cancer-related functions of CD44 in gastric cancer. *FEBS Lett* **2019**, *593*, 1675-1689, doi:10.1002/1873-3468.13432.
53. Rothenberg, S.M.; Ellisen, L.W. The molecular pathogenesis of head and neck squamous cell carcinoma. *J Clin Invest* **2012**, *122*, 1951-1957, doi:10.1172/jci59889.
54. Compagnone, M.; Gatti, V.; Presutti, D.; Ruberti, G.; Fierro, C.; Markert, E.K.; Vousden, K.H.; Zhou, H.; Mauriello, A.; Anemone, L.; et al. ΔNp63-mediated regulation of hyaluronic acid metabolism and signaling supports HNSCC tumorigenesis. *Proc Natl Acad Sci U S A* **2017**, *114*, 13254-13259, doi:10.1073/pnas.1711777114.
55. Orian-Rousseau, V.; Ponta, H. Perspectives of CD44 targeting therapies. *Arch Toxicol* **2015**, *89*, 3-14, doi:10.1007/s00204-014-1424-2.
56. Menke-van der Houven van Oordt, C.W.; Gomez-Roca, C.; van Herpen, C.; Coveler, A.L.; Mahalingam, D.; Verheul, H.M.; van der Graaf, W.T.; Christen, R.; Rüttinger, D.; Weigand, S.; et al. First-in-human phase I clinical trial of RG7356, an anti-CD44 humanized antibody, in patients with advanced, CD44-expressing solid tumors. *Oncotarget* **2016**, *7*, 80046-80058, doi:10.18632/oncotarget.11098.

Preprints (www.preprints.org) | NOT PEER-REVIEWED | Posted: 31 January 2023 doi:10.20944/preprints202301.0581.v1

57. Riechelmann, H.; Sauter, A.; Golze, W.; Hanft, G.; Schroen, C.; Hoermann, K.; Erhardt, T.; Gronau, S. Phase I trial with the CD44v6-targeting immunoconjugate bivatuzumab mertansine in head and neck squamous cell carcinoma. *Oral Oncol* **2008**, *44*, 823-829, doi:10.1016/j.oraloncology.2007.10.009.
58. Tijink, B.M.; Buter, J.; de Bree, R.; Giaccone, G.; Lang, M.S.; Staab, A.; Leemans, C.R.; van Dongen, G.A. A phase I dose escalation study with anti-CD44v6 bivatuzumab mertansine in patients with incurable squamous cell carcinoma of the head and neck or esophagus. *Clin Cancer Res* **2006**, *12*, 6064-6072, doi:10.1158/1078-0432.Ccr-06-0910.
59. Li, G.; Suzuki, H.; Ohishi, T.; Asano, T.; Tanaka, T.; Yanaka, M.; Nakamura, T.; Yoshikawa, T.; Kawada, M.; Kaneko, M.K.; et al. Antitumor activities of a defucosylated anti-EpCAM monoclonal antibody in colorectal carcinoma xenograft models. *Int J Mol Med* **2023**, *51*, doi:10.3892/ijmm.2023.5221.
60. Nanamiya, R.; Takei, J.; Ohishi, T.; Asano, T.; Tanaka, T.; Sano, M.; Nakamura, T.; Yanaka, M.; Handa, S.; Tateyama, N.; et al. Defucosylated Anti-Epidermal Growth Factor Receptor Monoclonal Antibody (134-mG(2a)-f) Exerts Antitumor Activities in Mouse Xenograft Models of Canine Osteosarcoma. *Monoclon Antib Immunodiagn Immunother* **2022**, *41*, 1-7, doi:10.1089/mab.2021.0036.
61. Kawabata, H.; Suzuki, H.; Ohishi, T.; Kawada, M.; Kaneko, M.K.; Kato, Y. A Defucosylated Mouse Anti-CD10 Monoclonal Antibody (31-mG(2a)-f) Exerts Antitumor Activity in a Mouse Xenograft Model of CD10-Overexpressed Tumors. *Monoclon Antib Immunodiagn Immunother* **2022**, *41*, 59-66, doi:10.1089/mab.2021.0048.
62. Kawabata, H.; Ohishi, T.; Suzuki, H.; Asano, T.; Kawada, M.; Suzuki, H.; Kaneko, M.K.; Kato, Y. A Defucosylated Mouse Anti-CD10 Monoclonal Antibody (31-mG(2a)-f) Exerts Antitumor Activity in a Mouse Xenograft Model of Renal Cell Cancers. *Monoclon Antib Immunodiagn Immunother* **2022**, doi:10.1089/mab.2021.0049.
63. Asano, T.; Tanaka, T.; Suzuki, H.; Li, G.; Ohishi, T.; Kawada, M.; Yoshikawa, T.; Kaneko, M.K.; Kato, Y. A Defucosylated Anti-EpCAM Monoclonal Antibody (EpMab-37-mG(2a)-f) Exerts Antitumor Activity in Xenograft Model. *Antibodies (Basel)* **2022**, *11*, doi:10.3390/antib11040074.
64. Tateyama, N.; Nanamiya, R.; Ohishi, T.; Takei, J.; Nakamura, T.; Yanaka, M.; Hosono, H.; Saito, M.; Asano, T.; Tanaka, T.; et al. Defucosylated Anti-Epidermal Growth Factor Receptor Monoclonal Antibody 134-mG(2a)-f Exerts Antitumor Activities in Mouse Xenograft Models of Dog Epidermal Growth Factor Receptor-Overexpressed Cells. *Monoclon Antib Immunodiagn Immunother* **2021**, *40*, 177-183, doi:10.1089/mab.2021.0022.
65. Takei, J.; Ohishi, T.; Kaneko, M.K.; Harada, H.; Kawada, M.; Kato, Y. A defucosylated anti-PD-L1 monoclonal antibody 13-mG(2a)-f exerts antitumor effects in mouse xenograft models of oral squamous cell carcinoma. *Biochem Biophys Rep* **2020**, *24*, 100801, doi:10.1016/j.bbrep.2020.100801.